Frontiers in Bioscience Landmark

Front. Biosci. (Landmark Ed) **2023**; 28(8): 162
https://doi.org/10.31083/j.fbl2808162

Original Research

Myc-Associated Zinc Finger Protein Promotes Metastasis of Papillary Thyroid Cancer

Chuanjun Zheng[1,†], Hongmei Wu[1,†], Shidong Zhang[1], Run Tian[1], Hu Long[1,2], Huixia Zhang[1], Xuefeng Guo[1], Di Li[1], Shengkui Tan[1,*], Xiaonian Zhu[1,*]

[1]Guangxi Key Laboratory of Environmental Exposomics and Entire Lifecycle Health, Guilin Medical University, 541199 Guilin, Guangxi, China
[2]Emergency Management Office, Guilin Center for Disease Control and Prevention, 541001 Guilin, Guangxi, China
*Correspondence: sktan2008@163.com (Shengkui Tan); zhuxiaonian0403@163.com (Xiaonian Zhu)
[†]These authors contributed equally.

Academic Editors: Francesca Bruzzese and Antonio Barbieri
Submitted: 8 December 2022 Revised: 18 January 2023 Accepted: 8 February 2023 Published: 11 August 2023

Abstract

Background: Myc-associated zinc finger protein (MAZ) plays a role in cancer progression and metastasis. However, the role and underlying molecular mechanism of MAZ in thyroid cancer have not yet been fully elucidated. This study aimed to explore the clinical significance of MAZ in thyroid cancer tissues, and clarify its mechanism in the occurrence and development of thyroid cancer. **Methods**: The expression level of MAZ protein in thyroid cancer tissues was detected by bioinformatics analysis and immunohistochemistry (IHC). The relationship between the expression level of MAZ and clinicopathological characteristics of thyroid cancer patients was analyzed by multivariate logistic regression analysis. Quantitative reverse-transcription polymerase chain reaction (RT-qPCR) was used to detect the mRNA expression level of MAZ in thyroid cancer cell lines. After MAZ knockdown cell lines were constructed, wound healing and Transwell assays were used to detect the migratory and invasive abilities of cancer cells. **Results**: The results of IHC showed that the expression level of MAZ protein in thyroid cancer tissues was higher than that in normal adjacent thyroid tissues ($p < 0.05$), which was consistent with the high expression level of MAZ in thyroid cancer tissues found in The Cancer Genome Atlas (TCGA) database. The results of multivariate logistic regression analysis indicated that the expression level of MAZ was correlated with tumor diameter and tumor capsule of thyroid cancer patients. Moreover, patients with the high MAZ expression level had shorter overall and disease-free survival compared with thyroid cancer patients with the low MAZ expression level ($p < 0.05$). Further cell function assays indicated that downregulation of MAZ expression level could inhibit the migration and invasion of thyroid cancer cell lines. Moreover, the expression level of epithelial-mesenchymal transition (EMT)-related factor fibronectin 1 (FN1) was obtained from the RNA-seq of MAZ knockdown in thyroid cancer cells. RT-qPCR confirmed that the expression level of FN1 was elevated in MAZ knockdown cell lines ($p < 0.05$). Bioinformatics analysis indicated that the expression level of FN1 was upregulated in thyroid cancer tissues and had a negative relationship with the expression level of MAZ, as evidenced by correlation analysis. **Conclusions**: A high expression level of MAZ in thyroid cancer tissues was associated with a poor prognosis of patients. MAZ could affect the progression of thyroid cancer by inducing the EMT process.

Keywords: MAZ; thyroid cancer; prognosis; EMT; FN1

1. Introduction

Among endocrine malignancies, thyroid cancer accounts for 3% of diagnosed cancer cases worldwide. Medullary thyroid cancer is a tumor arising from the parafollicular cells or C cells of the thyroid gland, accounting for 2–3% of cases with thyroid cancer [1]. The thyroid cancer mainly originates from follicular cells, which is subdivided into poorly differentiated thyroid cancer (PDTC), follicular thyroid cancer (FTC), anaplastic thyroid cancer (ATC), and papillary thyroid carcinoma (PTC) [2]. PTC and FTC are classified as differentiated thyroid carcinoma (DTC) [1]. In the 2004 guideline of the World Health Organization Classification of Tumors, PDTC was considered as a distinct subtype of thyroid cancer [3], in which its prognosis was between DTC and ATC, and it was typically reported in older patients [4]. Preoperative risk assessment determines the primary treatment for thyroid cancer. The majority of patients with thyroid cancer require surgery. Depending on the characteristics of the patient's disease, surgical modalities, such as lobectomy and total thyroidectomy with or without central cervical lymphatic dissection, are selected. Recurrent disease in DTC patients undergoing total thyroidectomy could be preventable and treatable with radioactive iodine (RAI). However, about 60–70% of PDTC patients and metastatic DTC patients may eventually develop to RAI-refractory (RAI-R) thyroid cancer [5]. The life expectancy of patients with RAI-R thyroid cancer is about 3 to 5 years [6]. ATC has the worst prognosis of follicular cells-derived malignancies, because it is typically diagnosed in an advanced metastatic stage, the primary tumor is large and rapidly grows, and complete resection is not always successful [7]. In addition, current treatment options

for ATC are limited, mainly involving multimodal therapy, *in vitro* high-dose radiotherapy, and surgery or chemotherapy at the same time [5]. A previous study has shown that although multimodal therapy could negatively affect the quality of life of patients with localized ATC, it might provide some survival benefits to them [8]. Therefore, understanding of the molecular mechanism of thyroid cancer is particularly important for developing further efficacious therapeutic approaches.

As a transcription factor with zinc finger domains, Myc-associated zinc finger protein (MAZ) has different regulatory effects on the transcriptional initiation of different genes. It can not only transactivate a great number of genes, such as the RAS gene family [9], platelet aggregation-inducing factor (podoplanin, PDPN) [10], caveolin-1 (CAV1) [11], and vascular endothelial growth factor (VEGF) [12], but also inhibit certain oncogenes, including proto-oncogene c-Myc [13], endothelial nitric oxide synthase [14], c-Myb [15], transcription factor SP4 [16], and telomerase [17]. The high expression level of MAZ in malignant tumors has been confirmed in some studies [12,18–22]. The interaction between MAZ and androgen receptor can promote the proliferation and metastasis of prostate cancer cells [14]. Franz *et al.* [23] found that combination of SPIN1 with MAZ could regulate the expression level of GDNF, thereby controlling the proliferation and apoptosis of human liposarcoma cells. Triner *et al.* [24] demonstrated that the expression level of MAZ could significantly promote the progression of colon cancer. It has also been shown that overexpression of MAZ could induce epithelial-mesenchymal transition (EMT) process in hepatocellular carcinoma (HCC), and it could be associated with the poor prognosis of HCC patients [20]. However, the functions and potential molecular mechanisms of MAZ in thyroid cancer have not yet been fully elucidated.

In the present study, the expression level of MAZ protein in thyroid cancer tissues was detected by immunohistochemistry (IHC), and the prognostic significance of MAZ in thyroid cancer was also analyzed. Furthermore, biological functions and molecular mechanisms of MAZ in thyroid cancer cells were explored through analyzing the expression level of MAZ. This study may provide a reliable basis for clinicians to treat thyroid cancer.

2. Materials and Methods

2.1 Bioinformatics Analysis

Analysis of differentially expressed genes (DEGs) in thyroid cancer and normal tissues was performed using gene expression profiling interactive analysis (GEPIA, http://gepia.cancer-pku.cn/index.html). The criteria were |log2FC| Cutoff: 1, *p*-value Cutoff: 0.01, THCA, Match TCGA normal and GTEx data, and 512 thyroid cancer tissue samples and 337 normal control tissue samples were included. The same method was used to analyze differences in the expression level of fibronectin 1 (FN1) between thyroid cancer tissues and normal tissues. The R package (version 3.4.4, Auckland, New Zealand) was used to divide samples into high expression and low expression groups according to the median expression level of MAZ, and they were then analyzed. Kaplan-Meier test was utilized to analyze the overall survival (OS) and disease-free survival (DFS) of thyroid cancer patients in The Cancer Genome Atlas (TCGA) database.

2.2 IHC and Scoring

A total of 58 pairs of paraffin-embedded papillary thyroid cancer tissue microarray chips were provided by Xinchao Company (Shanghai, China), which were routinely dried, dewaxed, hydrated, and the antigens were repaired under high pressure with citrate repair buffer in 3% hydrogen peroxide. The chips were soaked for 10 min to remove endogenous peroxidase. Then, goat serum was added for blocking for 20 min, diluted primary antibody (MAZ, #ab85725, 1:200; Abcam, Cambridge, UK) was added dropwise, and placed into a refrigerator at 4 °C overnight. On the next day, the secondary antibody (enzyme-labeled anti-mouse/rabbit IgG polymer) was added into drops and placed at room temperature for 30 min. Afterwards, 3,3′-diaminobenzidine (DAB) was added for developing the color, and visualization was performed under a microscope for 5–10 min until the appropriate color appeared. Finally, the chips were counterstained with hematoxylin, dehydrated, dried, and fixed.

All immunostained sections were double-blinded, and five fields of view were randomly selected under a high-magnification microscope for scoring. Staining intensity was scored according to the nuclear staining: 0 indicated no intensity, 1 indicated light intensity, 2 indicated medium intensity, and 3 indicated high intensity that was dark brown. More than 500 cells were counted to determine the percentage of immunostained cells in the total cells.

The percentage of positively stained cells was scored as follows: 0 ($\leq$5%), 1 (6–25%), 2 (26–50%), 3 (51–75%), and 4 (>75%). The product of the two scores was the final score of the staining. In the present study, a score of <4 was indicative of negative expression of MAZ, and a score of $\geq$4 was representative of positive expression of MAZ.

2.3 Cell Culture and Plasmid Transfection

Four thyroid cancer cell lines (human thyroid squamous cell carcinoma cell line SW579, human papillary thyroid cancer cell lines B-CPAP and TPC-1, and human anaplastic thyroid cancer cell line 8505C) were purchased and validated by STR authentication and mycoplasma test from Shanghai Yihe Application Biological Technology Co., Ltd. (Shanghai, China). The cells were cultured in a complete Dulbecco's modified Eagle's medium (DMEM), consisting of fetal bovine serum (FBS) and peni-

cillin/streptomycin mixture (Solarbio Science & Technology Co., Ltd., Beijing, China) in an 89:10:1 ratio. The growth conditions of the cells were 5% CO_2 in a 37 °C incubator.

Cells at the logarithmic growth phase were inoculated into six-well plates and transfected with liposome 2000 (Invitrogen, Carlsbad, CA, USA) according to the manufacturer's instructions when the cells reached a confluence of 80%. After 6 h of transfection, the cells were stored in a fresh medium for subsequent experiments.

2.4 RNA-seq and Quality Control

TRIzol reagent (Tiangen, Beijing, China) was used to extract the total RNA of thyroid cancer cell line 8505C after 48 h of transfection. Total RNA concentration was measured by Nanodrop 2000 (Thermo Fisher Scientific, Waltham, MA, USA). The transcriptome sequencing bioinformatics analysis was performed by GeneChem Co., Ltd. (Shanghai, China). The libraries were sequenced using a 150 bp double-ended sequencing strategy on the Illumina-HiSeq2000 platform. The raw imaging data were converted from sequence data generated by base calling (Illumina pipeline CASAVA ver. 1.8.2, Illumina Inc., San Diego, CA, USA). Then, quality control standards were used to remove reads that did not meet the following criteria: (1) readings are paired with joints and primers, at most two mismatches; (2) exceeding 5% of unknown bases at the time of reading; (3) over 50% of the low-quality bases. Finally, after quality control, filtered reads were retained for further analysis.

2.5 Analysis of DEGs

Analysis of DEGs in two groups (two biological replicates per group) was performed using DESeq2 (version 1.16.1, R package, Auckland, New Zealand). DESeq2 shares information across genes to generate more accurate estimates of variation based on the mean expression level of the gene. Benjamini-Hochberg method was adopted to adjust the p and control the false discovery rate. Using DESeq2, it was found that DEGs met $p < 0.05$ after adjustment. Corrected p and $|\log2FC|$ were used as thresholds for significant DEGs.

2.6 GO and KEGG Pathway Enrichment Analyses of DEGs

The Gene Ontology (GO) enrichment analysis of DEGs was performed by the clusterProfiler package of R 3.4.4 software, in which the gene length bias was corrected. GO terms with corrected $p < 0.05$ indicated significant DEGs. The Kyoto Encyclopedia of Genes and Genomes (KEGG) is a database enabling researchers to systematically analyze gene function and genomes. The clusterProfiler package of R 3.4.4 software was utilized to analyze DEGs in the KEGG pathway.

2.7 Quantitative Reverse-Transcription Polymerase Chain Reaction (RT-qPCR)

Total RNA was extracted using TRIzol reagent, and was then reversely transcribed into a cDNA template, and PCR was performed using the SYBR Green Mixture kit (Tiangen). The sequences of primers used for RT-qPCR are shown in **Supplementary Table 1**. The PCR reaction conditions were summarized as follows: denaturation at 95 °C for 10 min, extension at 95 °C for 15 s, and annealing at 65 °C for 60 s for 40 cycles. Relative RNA expression was calculated using the $2^{-\Delta\Delta Ct}$ method.

2.8 Western Blot

Cells were harvested and lysed using RIPA Lysis Buffer (Beyotime, Shanghai, China). The concentration of total protein was determined by BCA Protein Assay Kit (Beyotime). 10 µg of protein samples were subjected to SDS-PAGE. After that, PVDF membrane was incubated with MAZ and GAPDH (#AF0006, 1:1000; Beyotime) primary antibody to determine the protein expression of MAZ and GAPDH.

2.9 Cell Scratching Assay

Cells were cultured in 6-well plates. After 12 h of culture, the cells were scratched vertically in one direction with a 10 µL tip, and were then washed with phosphate-buffered saline (PBS) before adding fresh serum-free culture medium. The cells were observed and photographed under a microscope at 0, 24, and 48 h, respectively, and the cell migration was measured using ImageJ software (version 1.8.0, National Institutes of Health, Bethesda, MD, USA). The difference was determined between the scratching width with a mobility of 0 h minus the scratching width of 24 or 48 h and divided by the scratching width of 0 h.

2.10 Cell Invasion and Migration Assays

Transwell chambers (BD, Franklin Lakes, NJ, USA) with or without Matrigel were used to detect cell migration and invasion. Place the chamber into a 24-well plate, add culture medium, and incubate in an incubator for 30 min. Add 100 µL serum-free culture medium containing 2×10^4 cells to the upper chamber, and add 600 µL of culture medium with 10% FBS to the lower chamber. After 30 h, fix the cells with 4% paraformaldehyde for 40 min, and perform staining with 1% crystal violet for 1 h. After washing with PBS, wipe off the Matrigel and remaining cells with a cotton swab. Take a picture of the cells and count them.

2.11 Statistical Analysis

In the present study, SPSS 28.0 software (IBM, Armonk, NY, USA) was used to perform statistical analysis. The comparison between two groups was carried out by the Chi-square test. Multivariate logistic regression was used to analyze the relationship between the expression level of MAZ and clinicopathological features of patients with

thyroid cancer. Survival analysis was performed using the Kaplan-Meier method. The Spearman correlation test was used to analyze the correlation between the expression levels of MAZ and FN1 in thyroid cancer tissues. $p < 0.05$ was considered statistically significant.

3. Results

3.1 Expression Level of MAZ in Thyroid Cancer Tissues

In order to determine the expression level of MAZ in thyroid cancer tissues, bioinformatics analysis was initially conducted. In TCGA database, the expression level of MAZ in thyroid cancer tissues was significantly higher than that in the adjacent non-tumor tissues ($p < 0.05$, Fig. 1A). Then, to confirm the results of the bioinformatics analysis, 58 paired papillary thyroid cancer and adjacent non-tumor thyroid tissue samples were collected, and IHC was carried out. As shown in Fig. 1B, MAZ protein was mainly located in the nucleus and cytoplasm. The positive expression rate of MAZ in papillary thyroid cancer tissues was 75.86% (44/58), and the positive expression rate in the paired adjacent non-tumor tissues was 18.96% (11/58). The difference in the expression level of MAZ between papillary thyroid cancer and adjacent non-tumor tissues was statistically significant ($p < 0.001$, Table 1). The Wilcoxon test was used to compare the immunostaining scores of MAZ in papillary thyroid cancer and adjacent non-tumor tissues. The results showed that the MAZ staining scores in the adjacent non-tumor tissues were lower than those in the papillary thyroid cancer tissues. The median difference between the two groups was –3.5 (95% confidence interval (CI): –4~–2.5, $p < 0.001$, Fig. 1C). These results suggested that the expression level of MAZ was upregulated in papillary thyroid cancer tissues.

Table 1. MAZ expression in paired papillary thyroid cancer tissues and adjacent non-tumor tissues.

Thyroid cancer tissues	Adjacent normal tissues		Total
	Positive	Negative	
Positive	9	35	44
Negative	2	12	14
Total	11	47	58

Notes: $p < 0.001$. p-value is based on the McNemar χ^2 tests.

3.2 Relationship between Expression Level of MAZ and Prognosis of Patients with Thyroid Cancer

To further explore the effects of the expression level of MAZ on the prognosis of patients with thyroid cancer, the relationship between clinicopathological characteristics and the expression level of MAZ in 58 papillary thyroid cancer patients was clarified. Clinicopathological variables presented in Table 2 were included in the univariate analysis. The results showed that the expression level of MAZ

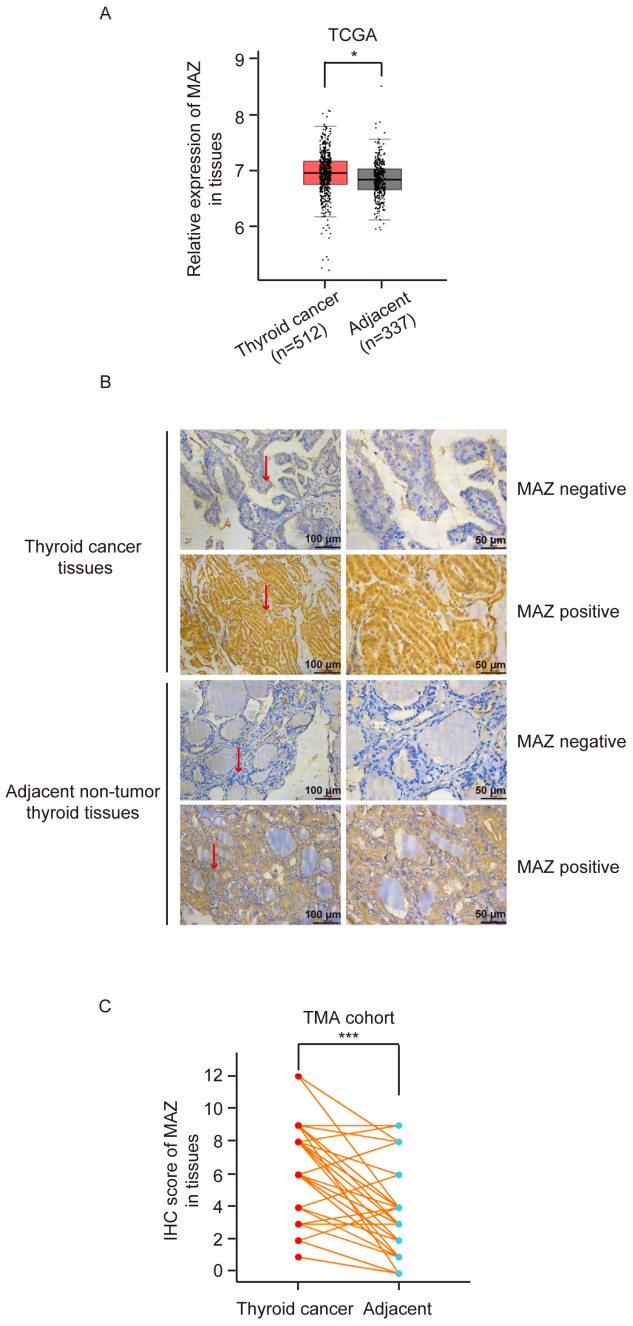

Fig. 1. Expression of MAZ in thyroid cancer tissues. (A) Expression of MAZ in thyroid cancer and adjacent tissues in TCGA database. (B) Representative results of immunohistochemical staining (red arrows indicate the position of image at ×400 magnification). (C) Staining score of MAZ in papillary thyroid cancer tissues and adjacent tissues (n = 58). *, $p < 0.05$, and ***, $p < 0.001$. MAZ, Myc-associated zinc finger protein; TCGA, The Cancer Genome Atlas.

was correlated with tumor, node, and metastasis (TNM) stage, tumor diameter, and tumor capsule ($p < 0.05$, Table 2). Then, variables with $p < 0.1$ in univariate analysis were imported into the multivariate logistic regression analysis. As a result, it was found that the expression level of

Table 2. Relationship between the expression of MAZ and clinicopathological features of papillary thyroid cancer patients.

Variables		Total	MAZ staining		χ^2	p
			Positive	Negative		
Gender						
	Male	23	17	6	0.079	0.779
	Female	35	27	8		
Age (year)						
	≥45	34	27	7	0.565	0.452
	<45	24	17	7		
Tumor stage						
	III+IV	18	17	1	-	**0.044**
	I+II	40	27	13		
Clinical stage						
	T3+T4	21	17	4	0.466	0.495
	T1+T2	37	27	10		
Tumor diameter (cm)						
	≥2.5	24	22	2	5.585	**0.018**
	<2.5	34	22	12		
Tumor location						
	Bilateral	10	7	3	-	0.691
	Unilateral/isthmus	48	37	11		
Tumor capsule						
	Yes	52	42	10	-	**0.026**
	No	6	2	4		
Lymph node metastasis						
	Yes	15	13	2	-	0.317
	No	43	31	12		

Notes: Bold values indicate significance.

MAZ was significantly associated with tumor diameter (OR = 6, 95% CI: 1.2~29.998, $p = 0.029$) and tumor capsule (OR = 8.4, 95% CI: 1.345~52.476, $p = 0.023$) (Table 3).

According to the clinical data downloaded from TCGA database, the Kaplan-Meier method was used to analyze the relationship between the expression level of MAZ and the prognosis of patients with thyroid cancer. According to the expression level of MAZ, all patients were divided into two groups. Compared with the low MAZ expression group, thyroid cancer patients in the high MAZ expression group had lower OS and DFS ($p < 0.05$, Fig. 2A,B). These results demonstrated that the expression level of MAZ was correlated with prognosis of thyroid cancer patients, indicating the role of the expression level of MAZ in thyroid cancer progression.

3.3 Downregulation of MAZ Inhibited the Invasive and Metastatic Abilities of Thyroid Cancer Cells

To investigate the biological functions of MAZ in thyroid cancer cells, the mRNA expression levels of MAZ in four thyroid cancer cell lines (SW579, B-CPAP, TPC-1, and 8505C) were detected by RT-qPCR. It is noteworthy that 8505C cell line was selected for the following experiment, because it had the highest MAZ mRNA expression level among the four cell lines (Fig. 3A). Two short hairpin RNAs (shRNAs) targeting MAZ were purchased from GeneChem Co., Ltd., including KD-1# and KD-2#, to knockdown the expression level of MAZ in cells. Two shRNAs were introduced into 8505C cells, and the expression level of MAZ in 8505C cells was detected after 48 h. Compared with the negative control (NC) group, both the mRNA and protein expression level of MAZ in the two groups (KD-1# or KD-2#) was significantly reduced ($p < 0.01$, Fig. 3B). Therefore, the two shRNAs could effectively interfere with the expression level of MAZ in thyroid cancer cells.

The migratory ability of 8505C cells with MAZ knockdown was detected by wound healing assay. Compared with the NC group, the cell migratory ability was significantly reduced after MAZ knockdown in the KD-1# and KD-2# groups, and the wound healing speed in the KD-1# group was slower than that in the KD-2# group ($p < 0.05$, Fig. 3C,D). The Transwell assay was performed in 8505C cells with MAZ knockdown to confirm MAZ role in metastasis of thyroid cancer cells. As shown in Fig. 3E,F, compared with the NC group, the invasive and migratory abilities in the KD1# and KD2# groups were significantly reduced, and the effect was more significant in the KD1#

Table 3. Multivariate logistic regression analysis for MAZ expression.

Variables	β	S.E.	Walds	p-value	OR	95% CI	
						Lower	Upper
Tumor stage	2.102	1.083	3.769	0.052	8.185	0.980	68.366
Tumor diameter	1.792	0.821	4.761	**0.029**	6.000	1.200	29.998
Tumor capsule	2.128	0.935	5.183	**0.023**	8.400	1.345	52.476

Notes: Bold values indicate significance. β, regression coefficient; S.E., standard error; OR, odd ratio; CI, confidence interval.

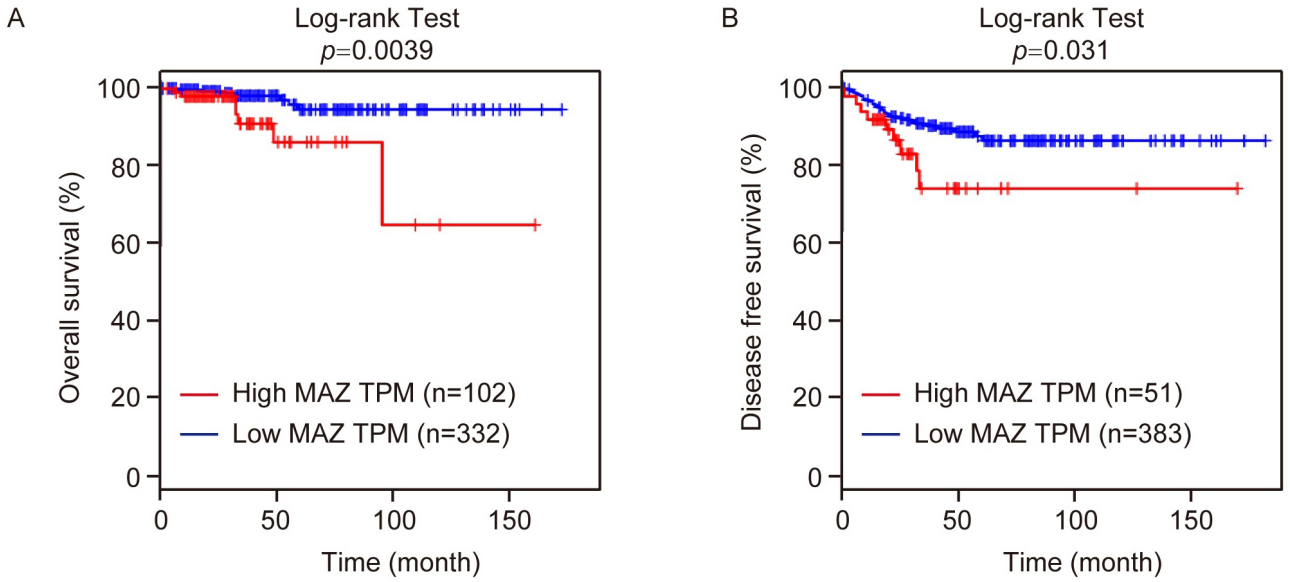

Fig. 2. Relationship between MAZ expression and thyroid cancer prognosis. (A) Kaplan-Meier plotter analysis of OS and (B) DFS of MAZ was conducted in patients with thyroid cancer. TPM, transcripts per million

group ($p < 0.05$). These results indicated that MAZ could play a role in the regulation of thyroid cancer metastasis.

3.4 GO and KEGG Pathway Enrichment Analyses Based on RNA-seq Data from MAZ Knockdown in Thyroid Cancer Cells

RNA sequencing of thyroid cancer cells after MAZ knockdown was performed using the GeneChip Human Gene 1.0 ST array. Then, according to the normalized expression levels, the correlation values between each sample were calculated and the correlation heat map was drawn. As shown in Fig. 4A, downregulation of MAZ changed the expression levels of various genes at the transcriptome level. Compared with the NC cells, there were 25,535 DEGs in MAZ knockdown cells, including 2129 upregulated genes and 2237 downregulated genes (Fig. 4B). To understand the relevant functions of DEGs in thyroid cancer after MAZ downregulation, GO enrichment analysis was conducted based on biological process (BP), cell component (CC), and molecular function (MF). The results indicated that MAZ-related DEGs were mainly enriched on ribonucleoprotein complex biogenesis, ribosome biogenesis, and rRNA metabolism in BP; in CC, they were mainly associated with focal adhesion, cell-substrate junction, and cell-substrate adhesion; in MF, they were mainly correlated with cadherin binding, structural composition of ribosomes, cell adhesion molecule binding, and mRNA binding (Fig. 4C). The results of KEGG pathway analysis showed that MAZ-related DEGs were mainly enriched in cancer pathway, neurotrophic factor signaling pathway, regulation of actin cytoskeleton, apoptosis pathway, protein processing in endoplasmic reticulum, and other pathways (Fig. 4D). The GO and KEGG pathway enrichment analyses further confirmed the involvement of MAZ in thyroid cancer progression.

3.5 MAZ Regulated the Expression Level of EMT-Related Factor FN1 in Thyroid Cancer

EMT-related factors participate in the metastatic progression of a great deal of malignant tumors. The expression level of EMT-related factor FN-1 was obtained from RNA-seq data of MAZ knockdown in thyroid cancer cells. The expression level of FN1 after MAZ downregulation was then examined to determine the EMT process. As shown in Fig. 5A, RT-qPCR assay showed that the expression level of FN1 was elevated in MAZ knockdosswn in thyroid cancer cells, and the expression level of FN1 in KD1# groups was higher than that in KD2# group ($p < 0.05$). Moreover, the expression level of MAZ in thyroid

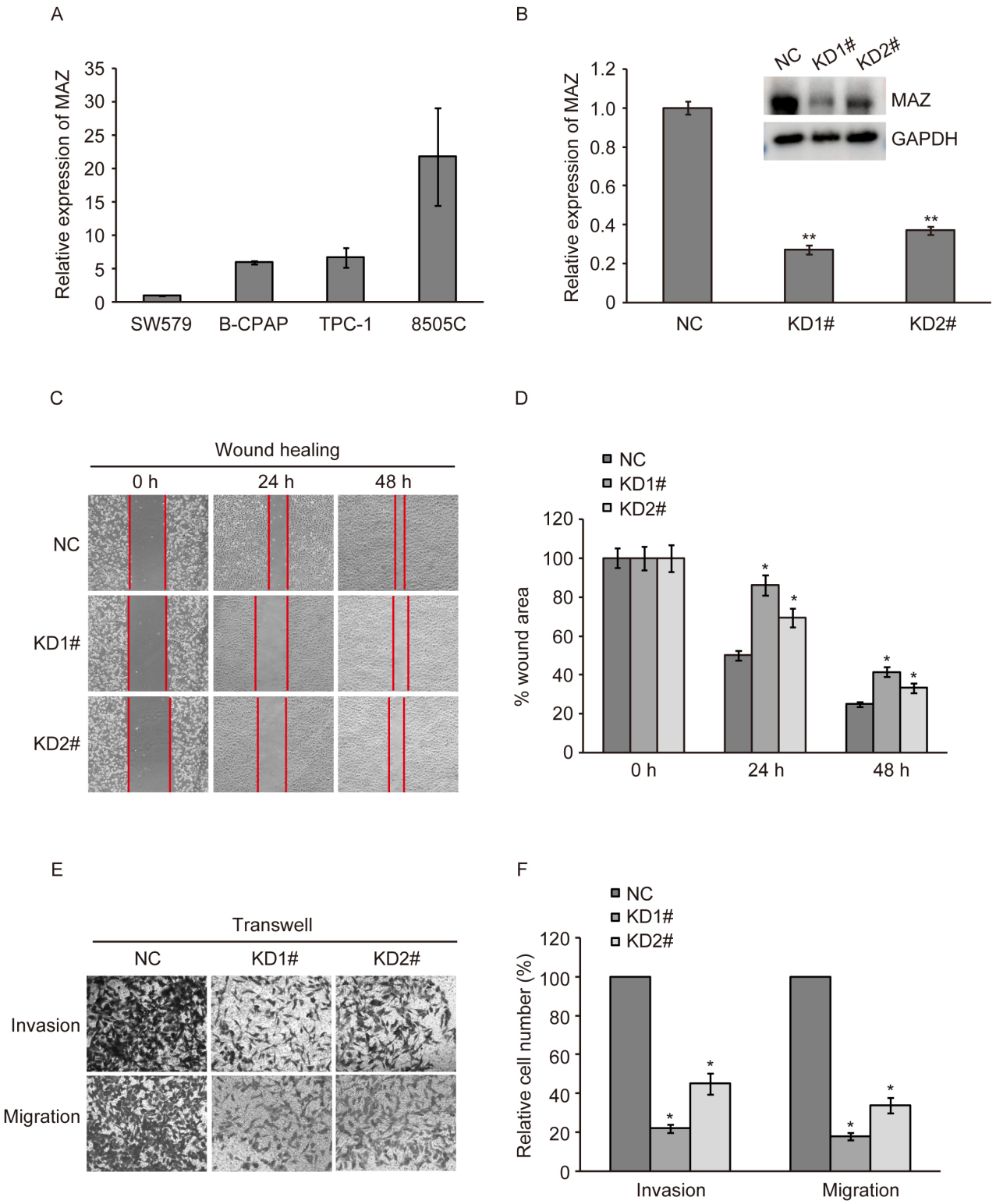

Fig. 3. Role of MAZ in metastasis of thyroid cancer. (A) RT-qPCR detection of relative expression of MAZ mRNA in thyroid cancer cell lines. (B) MAZ mRNA and protein expression after MAZ knockdown in 8505C cells. (C,D) Wound healing assay. (E,F) Transwell assay. *, $p < 0.05$, and **, $p < 0.01$. NC, negative control; KD, knock-down.

cancer tissues was negatively correlated with the expression level of FN1 (r = –0.31, $p < 0.001$, Fig. 5B). Data downloaded from TCGA database revealed that the expression level of FN1 in thyroid cancer tissues was higher than that in adjacent thyroid tissues ($p < 0.05$, Fig. 5C). These results indicated that MAZ may promote thyroid cancer metastasis through regulating the expression level of FN1.

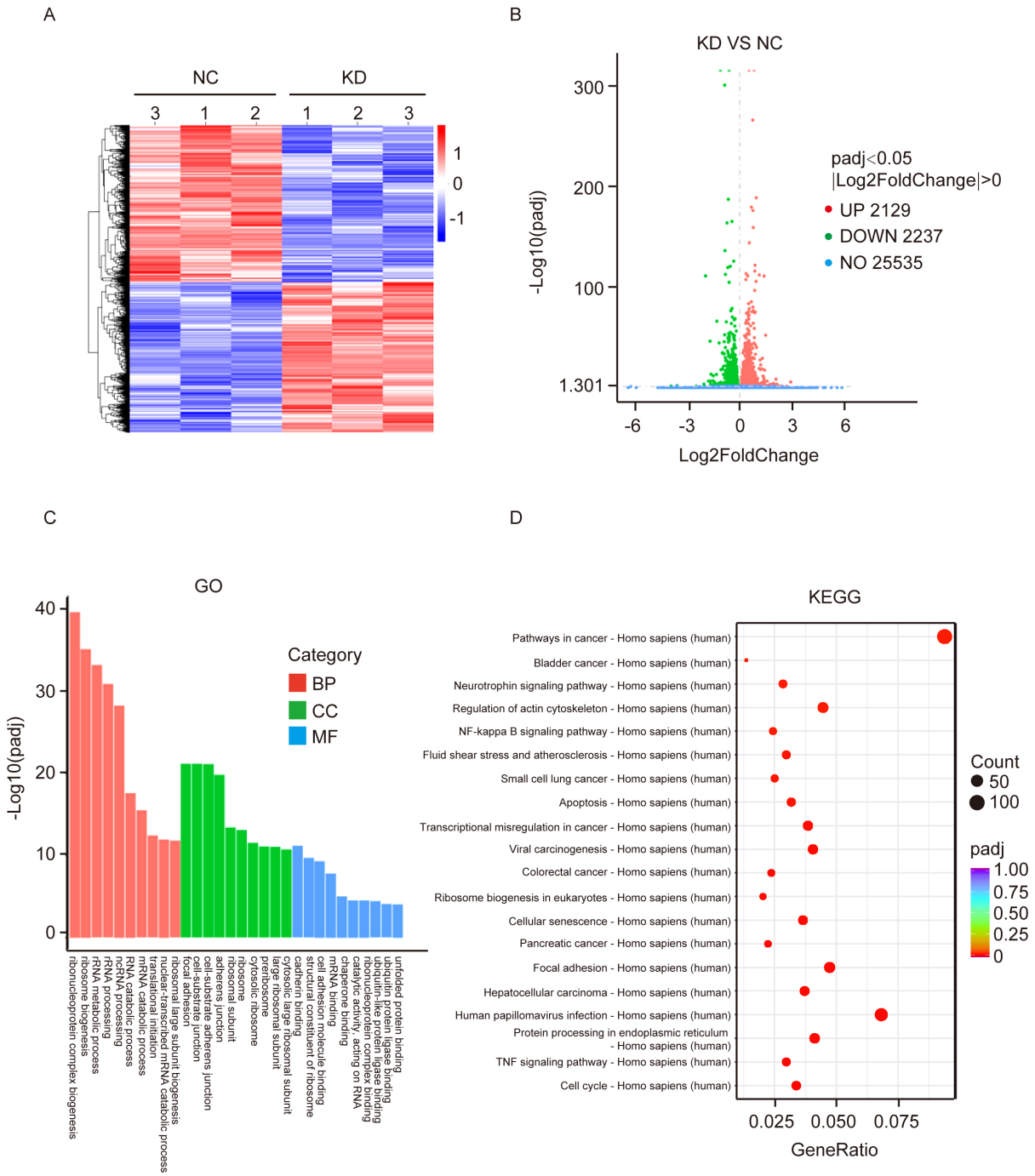

Fig. 4. RNA-seq results of MAZ knockdown thyroid cancer cells. (A) Heatmap of the differentially expressed genes (DEGs). (B) Volcano plot. (C) The Gene Ontology (GO) enrichment analysis. (D) The Kyoto Encyclopedia of Genes and Genomes (KEGG) enrich distribution point diagram. BP, biological process; CC, cell component; MF, molecular function.

4. Discussion

Thyroid cancer, as an endocrine malignant tumor, accounts for about 1% of human malignant tumors. Thyroid cancer can be treated by a variety of therapeutic approaches, such as surgery, RAI or chemotherapy, while its recurrence rate is still noticeable [25,26]. Therefore, exploration of potential prognostic markers for thyroid cancer patients is of great significance to improve patients' quality of life.

MAZ is a Cys-His-2 transcription factor that is widely expressed in different tissues of the human body [27]. It plays a dual regulatory role in transcription. Previous studies demonstrated that MAZ plays an integral role in the pathogenesis of triple-negative breast cancer [28,29]. A study also found that MAZ increased the activation of extracellular signal-regulated kinase (ERK) signaling pathway, and promoted renal clear cell carcinoma cell proliferation

Figure 5

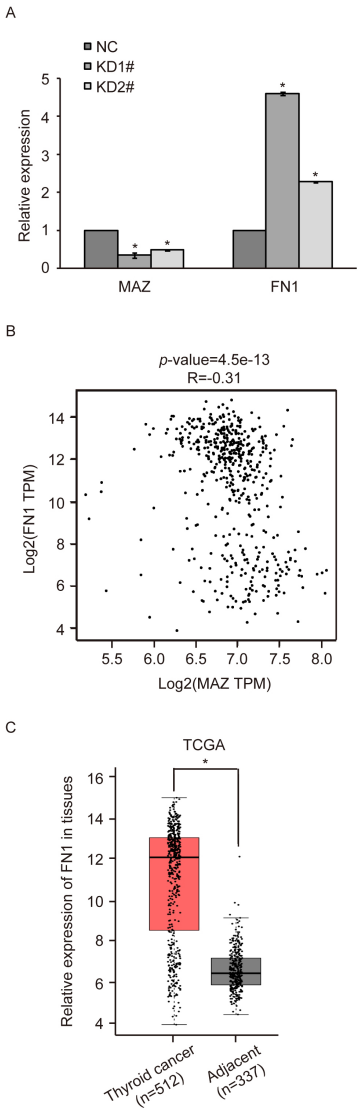

Fig. 5. Relationship between MAZ expression and FN1 expression in thyroid cancer. (A) RT-qPCR detection of relative expression of FN1 mRNA after MAZ down-regulation. (B) Correlation analysis between MAZ and FN1. (C) Expression of FN1 in thyroid cancer and adjacent tissues in TCGA database. *, $p < 0.05$. FN1, fibronectin 1.

[30]. Maity *et al.* [31] showed that the acquisition of the invasive phenotype of pancreatic ductal adenocarcinoma may be related to MAZ activation of CRAF-ERK signaling pathway. The interaction between MAZ and miR-29b-3p was found to have an impact on the migration and invasion of gastric cancer cells [32]. Overexpression of miR-149-3p inhibited the lung cancer cell migration and invasion by targeting MAZ [33]. These findings suggest that MAZ has the potential in current cancer therapy through regulating cancer cell proliferation and metastasis. However, the clinical significance and biological functions of MAZ in thyroid cancer should be further clarified.

In the present study, it was found that the expression level of MAZ was upregulated in thyroid cancer tissues by bioinformatics analysis and IHC. Combined with the analysis of clinicopathological data, it was revealed that the expression level of MAZ was significantly correlated with tumor diameter and tumor capsule, rather than with other clinicopathological features of papillary thyroid cancer patients. Moreover, thyroid cancer patients with a low MAZ expression level had longer OS and RFS, suggesting a poor prognosis of patients with a high MAZ expression level. To investigate MAZ-related cellular functions, validation experiments were performed. The results of wound healing and Transwell assays showed that downregulation of MAZ reduced the migratory and invasive abilities of thyroid cancer cells. The above-mentioned findings confirmed that in thyroid cancer, MAZ plays a role in promoting tumor growth.

To reveal the pathological function and underlying mechanism of MAZ in thyroid cancer development, RNA-seq of thyroid cancer cells after MAZ knockdown was performed. It was found that downregulation of MAZ changed the expression levels of various genes at the transcriptome level. There were 25,535 DEGs in MAZ knockdown cells, including 2129 upregulated DEGs and 2237 downregulated DEGs. The GO and KFGG pathway enrichment analyses of DEGs indicated that these DEGs were involved in the occurrence and development of thyroid cancer, such as focal adhesion, cell-substrate junction, cancer pathway, etc. Focal adhesion controls cell morphology, adhesion, and migration by linking the extracellular matrix with intercellular F-actin. Its ability to metastasize and invade is a key determinant of tumor resistance to treatment [34,35].

The expression level of EMT-related factor FN-1 was obtained from the RNA-seq of MAZ knockdown in thyroid cancer cells. FN1 is an extracellular matrix protein with multiple alternative splicing variants [36]. It regulates the interaction between cells and the extracellular matrix, and it is irreplaceable during cell growth, adhesion, differentiation, and migration [37,38]. Numerous studies have shown that FN1 is involved in oral squamous cell carcinoma [39], ovarian cancer [40], nasopharyngeal cancer [41], esophageal cancer [42], serous ovarian cancer [43], gastric cancer [44], and cervical cancer [45]. Different expression levels of FN1 exhibited different effects on tumor proliferation, migration, and invasion [46,47]. In the present study, bioinformatics analysis revealed that FN1 was highly expressed in thyroid cancer tissues. Moreover, the expression level of MAZ was negatively correlated with the expression level of FN1 in thyroid cancer tissues. Combined with the results of RT-qPCR assay after knockdown of MAZ, it was found that the expression level of MAZ could affect the expression level of FN1, and the two proteins were negatively correlated together. Collectively, downregulation of MAZ may inhibit the malignant progression

of thyroid cancer by inducing the EMT process. However, the specific mechanism remains to be further explored.

5. Conclusions

In conclusion, the upregulated expression level of MAZ in thyroid cancer tissues was found to be associated with the poor prognosis of patients, and downregulated expression level of MAZ could inhibit the migratory and invasive abilities of thyroid cancer cells by regulating the EMT process, suggesting that MAZ could play a role in promoting the development of thyroid cancer. Therefore, MAZ is expected to become a new early diagnostic marker and therapeutic target for thyroid cancer.

Availability of Data and Materials

The datasets used and analyzed during the current study are available from the corresponding authors on reasonable request.

Author Contributions

CZ, HW, XZ and ST designed the research study. CZ and HW performed the research. SZ, RT, HL, HZ, XG and DL analyzed the data. CZ, HW, XZ and ST wrote the manuscript. All authors contributed to editorial changes in the manuscript. All authors read and approved the final manuscript.

Ethics Approval and Consent to Participate

This study was approved by the Ethics Committee of Guilin Medical University (GLMC2020057), and the written informed consent of each patient participating in the study was obtained.

Acknowledgment

Not applicable.

Funding

This study was supported by the National Natural Science Foundation of China (81860586, 82060607, and 82060621), Natural Science Foundation of Guangxi Province (2020GXNSFDA297010) and the Graduate Student Joint Training Base Program of School of Public Health, Guilin Medical University (GWXY202006).

Conflict of Interest

The authors declare no conflict of interest.

Supplementary Material

Supplementary material associated with this article can be found, in the online version, at https://doi.org/10.31083/j.fbl2808162.

References

[1] Xing M. Molecular pathogenesis and mechanisms of thyroid cancer. Nature Reviews. Cancer. 2013; 13: 184–199.

[2] Molinaro E, Romei C, Biagini A, Sabini E, Agate L, Mazzeo S, *et al*. Anaplastic thyroid carcinoma: from clinicopathology to genetics and advanced therapies. Nature Reviews. Endocrinology. 2017; 13: 644–660.

[3] Sadow PM, Faquin WC. Poorly differentiated thyroid carcinoma: an incubating entity. Frontiers in Endocrinology. 2012; 3: 77.

[4] Ibrahimpasic T, Ghossein R, Shah JP, Ganly I. Poorly Differentiated Carcinoma of the Thyroid Gland: Current Status and Future Prospects. Thyroid. 2019; 29: 311–321.

[5] Filetti S, Durante C, Hartl D, Leboulleux S, Locati LD, Newbold K, *et al*. Thyroid cancer: ESMO Clinical Practice Guidelines for diagnosis, treatment and follow-up†. Annals of Oncology. 2019; 30: 1856–1883.

[6] Fugazzola L, Elisei R, Fuhrer D, Jarzab B, Leboulleux S, Newbold K, *et al*. 2019 European Thyroid Association Guidelines for the Treatment and Follow-Up of Advanced Radioiodine-Refractory Thyroid Cancer. European Thyroid Journal. 2019; 8: 227–245.

[7] Tiedje V, Stuschke M, Weber F, Dralle H, Moss L, Führer D. Anaplastic thyroid carcinoma: review of treatment protocols. Endocrine-related Cancer. 2018; 25: R153–R161.

[8] Fan D, Ma J, Bell AC, Groen AH, Olsen KS, Lok BH, *et al*. Outcomes of multimodal therapy in a large series of patients with anaplastic thyroid cancer. Cancer. 2020; 126: 444–452.

[9] Ray A, Ray BK. Induction of Ras by SAF-1/MAZ through a feed-forward loop promotes angiogenesis in breast cancer. Cancer Medicine. 2015; 4: 224–234.

[10] Yao Y, Ma J, Xue Y, Wang P, Li Z, Li Z, *et al*. MiR-449a exerts tumor-suppressive functions in human glioblastoma by targeting Myc-associated zinc-finger protein. Molecular Oncology. 2015; 9: 640–656.

[11] Xie L, Xue X, Taylor M, Ramakrishnan SK, Nagaoka K, Hao C, *et al*. Hypoxia-inducible factor/MAZ-dependent induction of caveolin-1 regulates colon permeability through suppression of occludin, leading to hypoxia-induced inflammation. Molecular and Cellular Biology. 2014; 34: 3013–3023.

[12] Smits M, Wurdinger T, van het Hof B, Drexhage JAR, Geerts D, Wesseling P, *et al*. Myc-associated zinc finger protein (MAZ) is regulated by miR-125b and mediates VEGF-induced angiogenesis in glioblastoma. FASEB Journal. 2012; 26: 2639–2647.

[13] Izzo MW, Strachan GD, Stubbs MC, Hall DJ. Transcriptional repression from the c-myc P2 promoter by the zinc finger protein ZF87/MAZ. The Journal of Biological Chemistry. 1999; 274: 19498–19506.

[14] Karantzoulis-Fegaras F, Antoniou H, Lai SL, Kulkarni G, D'Abreo C, Wong GK, *et al*. Characterization of the human endothelial nitric-oxide synthase promoter. The Journal of Biological Chemistry. 1999; 274: 3076–3093.

[15] Palumbo SL, Memmott RM, Uribe DJ, Krotova-Khan Y, Hurley LH, Ebbinghaus SW. A novel G-quadruplex-forming GGA repeat region in the c-myb promoter is a critical regulator of promoter activity. Nucleic Acids Research. 2008; 36: 1755–1769.

[16] Song J, Mangold M, Suske G, Geltinger C, Kanazawa I, Sun K, *et al*. Characterization and promoter analysis of the mouse gene for transcription factor Sp4. Gene. 2001; 264: 19–27.

[17] Su JM, Lai XM, Lan KH, Li CP, Chao Y, Yen SH, *et al*. X protein of hepatitis B virus functions as a transcriptional corepressor on the human telomerase promoter. Hepatology. 2007; 46: 402–413.

[18] Zaytseva YY, Wang X, Southard RC, Wallis NK, Kilgore MW. Down-regulation of PPARgamma1 suppresses cell growth and induces apoptosis in MCF-7 breast cancer cells. Molecular Cancer. 2008; 7: 90.
[19] Jiao L, Li Y, Shen D, Xu C, Wang L, Huang G, *et al*. The prostate cancer-up-regulated Myc-associated zinc-finger protein (MAZ) modulates proliferation and metastasis through reciprocal regulation of androgen receptor. Medical Oncology. 2013; 30: 570.
[20] Luo W, Zhu X, Liu W, Ren Y, Bei C, Qin L, *et al*. MYC associated zinc finger protein promotes the invasion and metastasis of hepatocellular carcinoma by inducing epithelial mesenchymal transition. Oncotarget. 2016; 7: 86420–86432.
[21] Li H, Yang F, Hu A, Wang X, Fang E, Chen Y, *et al*. Therapeutic targeting of circ-CUX1/EWSR1/MAZ axis inhibits glycolysis and neuroblastoma progression. EMBO Molecular Medicine. 2019; 11: e10835.
[22] Wang Y, Sun L, Qiu W, Qi W, Qi Y, Liu Z, *et al*. Inhibiting Forkhead box K1 induces autophagy to reverse epithelial-mesenchymal transition and metastasis in gastric cancer by regulating Myc-associated zinc finger protein in an acidic microenvironment. Aging. 2020; 12: 6129–6150.
[23] Franz H, Greschik H, Willmann D, Ozretić L, Jilg CA, Wardelmann E, *et al*. The histone code reader SPIN1 controls RET signaling in liposarcoma. Oncotarget. 2015; 6: 4773–4789.
[24] Triner D, Castillo C, Hakim JB, Xue X, Greenson JK, Nuñez G, *et al*. Myc-Associated Zinc Finger Protein Regulates the Proinflammatory Response in Colitis and Colon Cancer via STAT3 Signaling. Molecular and Cellular Biology. 2018; 38: e00386-18.
[25] Lang BHH, Lo CY, Wong KP, Wan KY. Should an involved but functioning recurrent laryngeal nerve be shaved or resected in a locally advanced papillary thyroid carcinoma? Annals of Surgical Oncology. 2013; 20: 2951–2957.
[26] Wang S, Wu J, Ren J, Vlantis AC, Li MY, Liu SYW, *et al*. MicroRNA-125b Interacts with Foxp3 to Induce Autophagy in Thyroid Cancer. Molecular Therapy. 2018; 26: 2295–2303.
[27] Ren J, Guo D, Wang X, Zhang C, Wang B, Gao Z. Revealing the alternative promoter usage of SAF/MAZ gene by bichromatic fluorescent reporter construct. Bioscience Reports. 2019; 39: BSR20171668.
[28] Peurala H, Greco D, Heikkinen T, Kaur S, Bartkova J, Jamshidi M, *et al*. MiR-34a expression has an effect for lower risk of metastasis and associates with expression patterns predicting clinical outcome in breast cancer. PLoS ONE. 2011; 6: e26122.
[29] Ray A, Dhar S, Ray BK. Control of VEGF expression in triple-negative breast carcinoma cells by suppression of SAF-1 transcription factor activity. Molecular Cancer Research. 2011; 9: 1030–1041.
[30] Ren LX, Qi JC, Zhao AN, Shi B, Zhang H, Wang DD, *et al*. Myc-associated zinc-finger protein promotes clear cell renal cell carcinoma progression through transcriptional activation of the MAP2K2-dependent ERK pathway. Cancer Cell International. 2021; 21: 323.
[31] Maity G, Haque I, Ghosh A, Dhar G, Gupta V, Sarkar S, *et al*. The MAZ transcription factor is a downstream target of the oncoprotein Cyr61/CCN1 and promotes pancreatic cancer cell invasion via CRAF-ERK signaling. The Journal of Biological Chemistry. 2018; 293: 4334–4349.
[32] Zhao X, Ye N, Feng X, Ju H, Liu R, Lu W. MicroRNA-29b-3p Inhibits the Migration and Invasion of Gastric Cancer Cells by Regulating the Autophagy-Associated Protein MAZ. OncoTargets and Therapy. 2021; 14: 3239–3249.
[33] Jiang Z, Ma Y, Tian T, Sun Y, Chen H, Lu Y, *et al*. Maimendong and Qianjinweijing Tang (Jin formula) suppresses lung cancer by regulation of miR-149-3p. Journal of Ethnopharmacology. 2020; 258: 112836.
[34] Matsuyama R, Okuzaki D, Okada M, Oneyama C. MicroRNA-27b suppresses tumor progression by regulating ARFGEF1 and focal adhesion signaling. Cancer Science. 2016; 107: 28–35.
[35] Liang R, Wang M, Zheng G, Zhu H, Zhi Y, Sun Z. A comprehensive analysis of prognosis prediction models based on pathway level, gene level and clinical information for glioblastoma. International Journal of Molecular Medicine. 2018; 42: 1837–1846.
[36] ffrench-Constant C. Alternative splicing of fibronectin–many different proteins but few different functions. Experimental Cell Research. 1995; 221: 261–271.
[37] Pankov R, Yamada KM. Fibronectin at a glance. Journal of Cell Science. 2002; 115: 3861–3863.
[38] Zollinger AJ, Smith ML. Fibronectin, the extracellular glue. Matrix Biology. 2017; 60–61: 27–37.
[39] Yen CY, Huang CY, Hou MF, Yang YH, Chang CH, Huang HW, *et al*. Evaluating the performance of fibronectin 1 (FN1), integrin $\alpha 4\beta 1$ (ITGA4), syndecan-2 (SDC2), and glycoprotein CD44 as the potential biomarkers of oral squamous cell carcinoma (OSCC). Biomarkers. 2013; 18: 63–72.
[40] Lou X, Han X, Jin C, Tian W, Yu W, Ding D, *et al*. SOX2 targets fibronectin 1 to promote cell migration and invasion in ovarian cancer: new molecular leads for therapeutic intervention. Omics. 2013; 17: 510–518.
[41] Ma LJ, Lee SW, Lin LC, Chen TJ, Chang IW, Hsu HP, *et al*. Fibronectin overexpression is associated with latent membrane protein 1 expression and has independent prognostic value for nasopharyngeal carcinoma. Tumour Biology. 2014; 35: 1703–1712.
[42] Li M, Wang K, Pang Y, Zhang H, Peng H, Shi Q, *et al*. Secreted Phosphoprotein 1 (SPP1) and Fibronectin 1 (FN1) Are Associated with Progression and Prognosis of Esophageal Cancer as Identified by Integrated Expression Profiles Analysis. Medical Science Monitor. 2020; 26: e920355.
[43] Liang H, Yu M, Yang R, Zhang L, Zhang L, Zhu D, *et al*. A PTAL-miR-101-FN1 Axis Promotes EMT and Invasion-Metastasis in Serous Ovarian Cancer. Molecular Therapy Oncolytics. 2019; 16: 53–62.
[44] Jiang K, Liu H, Xie D, Xiao Q. Differentially expressed genes *ASPN, COL1A1, FN1, VCAN* and *MUC5AC* are potential prognostic biomarkers for gastric cancer. Oncology Letters. 2019; 17: 3191–3202.
[45] Wang S, Gao B, Yang H, Liu X, Wu X, Wang W. MicroRNA-432 is downregulated in cervical cancer and directly targets FN1 to inhibit cell proliferation and invasion. Oncology Letters. 2019; 18: 1475–1482.
[46] Cai X, Liu C, Zhang TN, Zhu YW, Dong X, Xue P. Down-regulation of FN1 inhibits colorectal carcinogenesis by suppressing proliferation, migration, and invasion. Journal of Cellular Biochemistry. 2018; 119: 4717–4728.
[47] Xie Y, Liu C, Qin Y, Chen J, Fang J. Knockdown of IRE1α suppresses metastatic potential of colon cancer cells through inhibiting FN1-Src/FAK-GTPases signaling. The International Journal of Biochemistry & Cell Biology. 2019; 114: 105572.